

Impact of Moisture Buffering Effect in the Calibration of Historical Buildings Energy Models: A Case Study

*Harold Enrique Huerto-Cardenas^{*1}, Fabrizio Leonforte¹, Claudio Del Pero¹, Nicolò Aste¹, Michela Buzzetti¹, Rajendra Singh Adhikari¹, Alessandro Miglioli¹*

¹Department of architecture, built environment and construction engineering, Politecnico di Milano, Italy

e-mail: haroldenrique.huerto@polimi.it, fabrizio.leonforte@polimi.it, claudio.delpero@polimi.it, niccolo.aste@polimi.it, michela.buzzetti@polimi.it, rajendra.adhikari@polimi.it, alessandro.miglioli@polimi.it

Cite as: Huerto-Cardenas, H. E., Leonforte, F., Del Pero, C., Aste, N., Buzzetti, M., Singh Adhikari, R., Miglioli, A., Impact of moisture buffering effect in the calibration of historical buildings energy models: a case study, *J. sustain. dev. energy water environ. syst.*, 9(3), 1080370, 2021, DOI: <https://doi.org/10.13044/j.sdewes.d8.0370>

ABSTRACT

Building simulation software can provide a reliable prediction of the building environmental response, however, in historical building simulations the uncertainty increases due to the lack of information and the incorrect choice of the numerical model. In this work, the moisture buffering effect is investigated using two different models in EnergyPlus software. The analysis shows that the selection of the moisture buffering calculation method highly affects the simulation results and the set-up of some input variables during the calibration phase. In detail, the use of the Effective Capacitance model could overestimate the effects of the infiltration in terms of mixing ratio, leading to the adoption of a lower value of air change rate for the model validation (about 3 times in the case study analysed). Such phenomena particularly affect historical buildings, generally characterized by massive structures and many furnishings.

KEYWORDS

Historical buildings, Building energy simulation, Calibration, Moisture buffering, EMPD.

INTRODUCTION

Historical buildings are complex systems, expressions of material knowledge, unique resources worth to be preserved and enhanced by our society.

Looking at the state of the art of building heritage, currently, almost 5,367,000 belong to the world wide monuments UNESCO list [1] and, most of them are more than 50 years old. In particular, more than 40% of the European residential buildings have been constructed before the 1960s and more than 50% before the 1970s [2]. From an energy point of view, such buildings are responsible for 68% of the total final energy use, mainly related to heating, cooling, hot water, cooking and appliances [1]. In such respect in the last 20 years, the interest in a sustainable conversion and management of buildings is constantly increased [3, 4].

In such a framework, software traditionally used to estimate new buildings performances during the preliminary design phase has also been used in the heritage field to [5, 6]:

- analyse the possible risks to materials caused by specific environmental temperature and relative humidity conditions;

* Corresponding author

- estimate some phenomena that cannot be easily evaluated, for example, verification of surface condensation, etc.;
- analyse intervention (retrofit) scenarios according to different boundary conditions.

Building dynamic simulation tools represent a suitable mean for accurately assessing buildings thermal-energy performance, since they may be able to realistically predict the building behaviour in dynamic conditions. However, they are more time-intensive, need complex data inputs, require a certain period of user training and are not specifically designed for historical buildings. In general, a discrepancy (gap) between simulated and real behaviour can be observed for every building [7]; however, in historical buildings, the evidence related to the gap is presently too wide to be acceptable [8, 9].

In this context, the accuracy of building energy simulation (BES) models is an important issue that can be achieved through the so-called calibration process defined as the “process of reducing the uncertainty of a model by comparing the predicted output of the model under a specific set of conditions to the actual measured data for the same set of conditions” [10], since differences between the predicted and real energy performance can be significant [11, 12]. Generally, the (systematic) errors are attributable mainly to two causes Energy retrofits in historic and traditional buildings: A review of problems and methods [13, 14]. The first one is related to the use of incorrect data as input parameters, which generally comes from wrong measures, inappropriate assumptions or unpredictable user behaviour, which highly affects the simulation results [15]. The second is related to the calculation limitations of the tools which employ a wrong or incomplete model of the physical process that often occurs in historical and traditional buildings, e.g. envelope moisture buffering effect, thermal stratification in large spaces, etc. [16]. While the first cause of errors has been previously addressed [5], the latter is often neglected in the model calibration stage. Among the several simplifications often carried out in building energy simulations (BES), the effect of the moisture buffering is often oversimplified or even neglected, with the consequence to bring much inaccuracy to the simulation results [17]. However, even if different research works [18–20] demonstrate the significant impact of the moisture storage capacity of materials on the indoor humidity, none of them deeply focused on historical buildings, which are generally characterized by a high water retention capacity.

At the moment, although building dynamic simulation tools are potentially a suitable way for accurately assessing the performance of buildings, the results are highly affected by the capability of the user to select the most suitable method which well represents physical phenomena. Different methods are available for modelling moisture in BES [21].

Considering for example EnergyPlus, which represent one of the most commonly used tools by the research community for energy and environmental analysis [22], three different models, namely Effective Capacitance (EC), Effective Moisture Penetration Depth (EMPD) and Heat and Moisture Transfer (HAMT) can be adopted [17, 23]. Both the EC and the EMPD should be considered simplified models since the diffusion resistance and moisture capacity of the humidity buffer is considered constant and evaluated at average indoor humidity conditions [24]. However, the EC model is not able to accurately predict indoor humidity neither to provide a quantification of the moisture contents, since it works lumping the buffering effect with that of moisture capacitance of the zone air [25]. Furthermore, such simplified model is not able to predict the initial fast response of indoor humidity to changes in moisture production, compared to the other two models [24]. Nevertheless, since EC is the default model of EnergyPlus, it is still the most adopted method in building energy simulation according to the scientific literature.

The EMPD and HAMT models, on the contrary, are more reliable even if the moisture properties of the building materials are essential input, unlike in the EC model [23]. More in detail, the HAMT model is able to take into account and describe the mass transfer through the building components. However, it requires a greater amount of input parameters and computational time compared to the EMPD. In such respect, when only the impact of moisture

on the whole building response is of interest, this can be done by using simplified models for moisture transfer and storage, such as the EMPD [24], which has been shown to be accurate when appropriate inputs are provided [21].

In such a framework, the present work aims to analyse in detail the impact of EC and EMPD algorithms on the calibration of energy-environmental simulation models of historical buildings, typically characterized by a massive envelope with a high moisture capacitance and by the presence of furniture and artworks made with hygroscopic materials. In particular, the analysis has been carried out through the model calibration of an Italian historical building which is characterized by constant air infiltration, no internal gains and free-floating behaviour, which allows studying accurately such phenomenon. The case study is represented by the Palazzo Ducale of Mantua, one of the city's most important historical buildings.

The final objective of the work is to make aware researchers and energy experts involved in the conservation of heritage buildings of the reliability of different moisture buffering models in BES.

METHOD

The selection of the proper buffering model in energy simulation of historical buildings must be considered a pivotal part of the calibration in order to obtain reliable results.

In such respect, in the present study, the evaluation of the moisture buffering effect on the calibration of BES models was carried out with EnergyPlus, which represent the main reference software for the international building energy analysis community. Firstly, a baseline model developed with Effective Capacitance has been carried out. The required input parameters were set according to the data collected during a survey phase.

A specific weather file with actual data was defined and used for the model calibration since the outdoor climate conditions play an important role in the assessment of the environmental and energy performance of buildings. In such respect, the hourly data was collected from the nearby weather stations of the ARPA (Regional Environmental Protection Agency).

The simulated results were then compared with the real data acquired from a yearly on-site monitoring campaign. In particular, the calibration was performed considering the air infiltration rate that minimizes the mean bias error (*MBE*), mean absolute error (*MAE*), root mean squared error (*RMSE*) and optimizes the coefficient of determination (R^2), between simulated and measured indoor air temperature (*T*) and mixing ratio (*MR*). However, the present work will describe in detail the calibration process of the *MR* parameter, since the goal is to evaluate how the moisture buffering affect the model calibration with two different EnergyPlus algorithms.

The first three statistical indices adopted, are able to estimate the mean discrepancy between simulations and measurements, while, the last one (R^2) evaluate how much the model fits the actual building behaviour. The strength of combining different statistical indices instead of using them independently is stressed by different authors [26, 27], due to their ability to highlight different aspects of the results.

In detail, the *MBE* is calculated from the sum of the deviations between the measured and simulated data, dividing the result by the number of data points. The positive and negative result indicates respectively an under and overestimation of the simulated data compared to the measured ones. Since the *MBE* can be subject to the phenomenon of error cancellation [28], it should be used together with other indices. The *MAE* [29] takes into account the average absolute error of the differences between measured and predicted values (residuals), while the *RMSE* [30] represents the standard deviation of the differences between measured and simulated data. Compared to *MAE*, the *RMSE* is particularly sensitive to the amplitude of the residuals. Both *RMSE* and *MAE* are always positive and higher are their results, lower is the reliability of the simulation model.

The indices above mentioned providing results with the same measure unit of the adopted data, therefore, since in this work the model calibration is carried out through temperature and mixing ratio, the discrepancy will be estimated in terms of °C and g/kg respectively.

Finally, the R^2 coefficient is calculated to determine how well the model fits the measured data. This index assumes values ranging from 0 to 1, where 1 means that the model fits perfectly with the measured data. About the R^2 , the ASHRAE guideline 14 [31] and IPMVP [32], recommend values higher than 0.75. In detail, such indices are calculated according to the equations below:

$$MBE = \frac{\sum_{i=1}^n (m_i - s_i)}{n} \quad (1)$$

$$MAE = \frac{\sum_{i=1}^n |m_i - s_i|}{n} \quad (2)$$

$$RMSE = \sqrt{\frac{\sum_{i=1}^n (m_i - s_i)^2}{n}} \quad (3)$$

$$R^2 = 1 - \frac{\sum_{i=1}^n (m_i - s_i)^2}{\sum_{i=1}^n (m_i - \bar{m})^2} \quad (4)$$

where m_i and s_i are respectively the measured and simulated values, \bar{m} represent the mean of the measured data and n is the number of data points. Regarding the model reliability, the indices' thresholds adopted are those suggested by Huerto-Cardenas *et al.* [33]: ≤ 2 °C (T) and ≤ 2 g/kg (MR) for $RMSE$, and > 0.75 for R^2 .

Subsequently, the default algorithm was changed with the EMPD model to consider the effect of moisture buffering on the surfaces of the construction materials.

In such respect, the absence of internal surface condensation during the analysed year was verified to exclude the phase changes of the water vapour present in the air, which can affect the hygrometric balance. Moreover, it should be noted that the possible water accumulated into the building components, due to the rain is not considered in this analysis.

The results obtained from EMPD were compared with the previous simulations in order to highlight the main differences. A new calibration of the virtual model has been carried out, changing the infiltration rate to find out the value that optimizes the two selected metrics, according to the EMPD numerical model. Finally, in the context of conservation of cultural heritage, the ability of the simulation model of reproducing realistic daily fluctuations of MR has been evaluated.

In such respect, bridging the gap between predicted and measured performance is pivotal in order to provide a reliable evaluation of building performance to designers, architects, buildings' owners and policy makers.

In figure hereafter, a flow chart that describes the method adopted in this study has been reported.

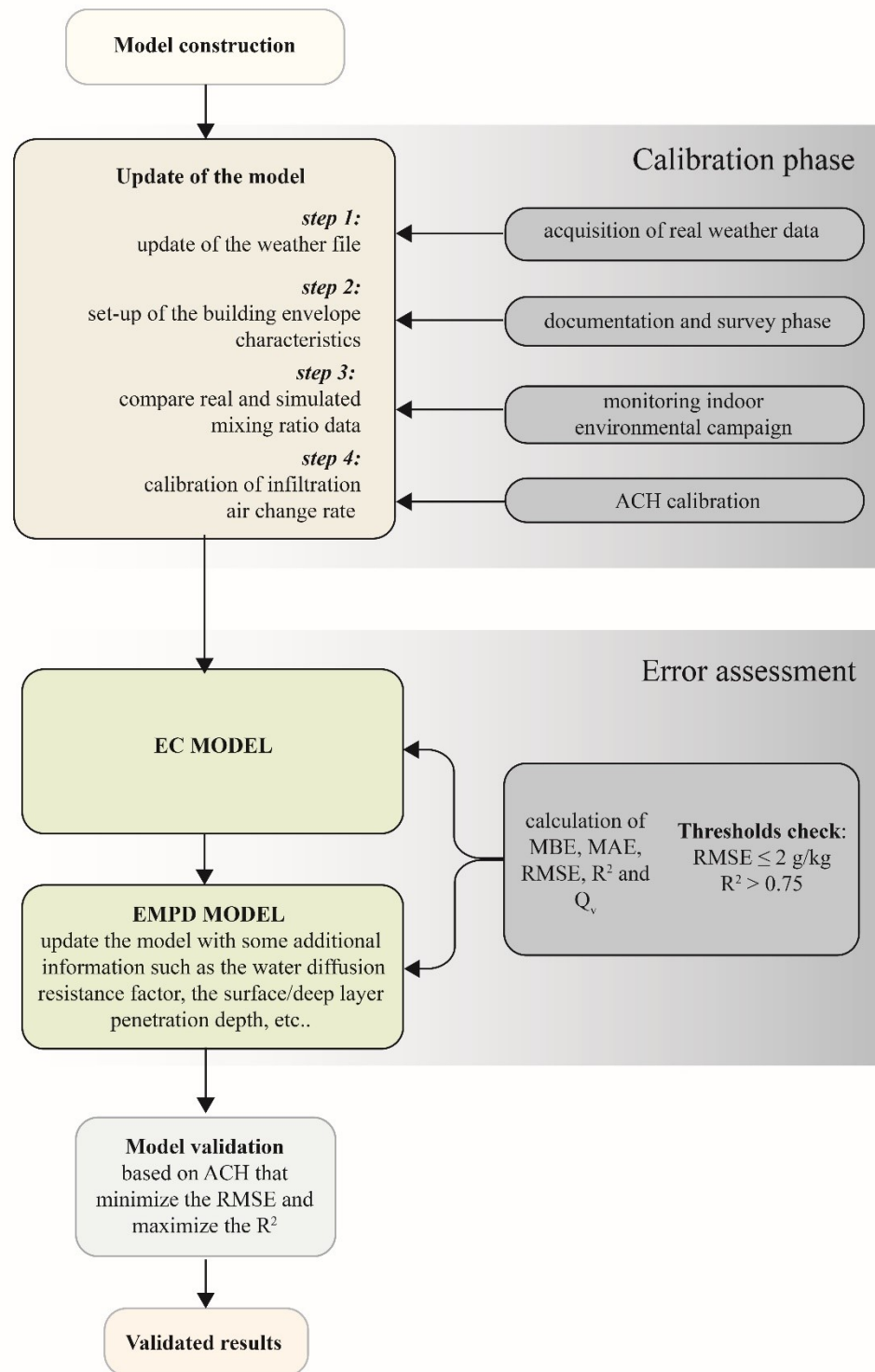


Figure 1. The method adopted in the study carried out

CASE STUDY

In this section are described the main features of the building case study, the environmental monitoring campaign carried out and the characteristics and assumptions of the BES model.

Case study description and building model

The selected space for this study is the Salone dell'Armeria, built in the 13th century and located in the Palazzo del Capitano, part of the enormous museum complex of the Palazzo

Ducale in Mantua (**Figure 2**). This hall is a single rectangular space that covers an area of about 1000 m² (66 m×15 m) with a maximum height of 11 m, for a total volume of approximately 9700 m³. The interior space is subdivided by transversal brick walls built in the 20th century.

Currently, the room is empty and no Heating Ventilation and Air Conditioning (HVAC) system are installed. Moreover, since this hall is not used and not accessible to visitors, during the year there are no people, electrical equipment and lights which could affect the internal heat and moisture balance. This particular condition has facilitated the calibration procedure of the building simulation model and allowed to exclude some variables for the assessment of the moisture buffering effect. The access is only allowed in extraordinary cases to technicians or researchers.

The external walls have a thickness that varies from 70 to 80 cm, made by solid bricks and the floor and the roof are realized with wooden structures. Thirteen double lancet windows, composed of single glasses and wooden frames, illuminate the indoor space.



Figure 2. View of Palazzo del Capitano from Piazza Sordello

Since Palazzo Ducale is a huge building complex, only the portion called “Palazzo del Capitano” that includes the space of the “Salone dell’Armeria” was modelled (**Figure 3**) [34]. The building geometry has been based on architectural drawings and collected documents. The thermal properties of the construction materials were selected from standards [35, 36] and literature [5, 37]. In detail, the thermal conductivity and the density of the walls made by bricks were defined considering a pre-industrial brick (from a period between 13th-18th Centuries) [5], while the thermal properties of single-glazed windows were selected from the literature [37]. The calculated *U*-values of the envelope components are shown in **Table 1**.

Table 1. *U*-values of the building envelope components

Building component	Material	<i>U</i> -value (W/m ² K)
Exterior wall	Solid bricks (from 70 to 80 cm)	0.57
Roof	Wood + tiles (10 cm + 1,5 cm)	0.87
Floor	Wood (15 cm)	0.95
Windows	Single-glazed (SHGC= 0.8)	5.71

Two main boundary conditions have been set in the thermal zones model: one for the Salone dell'Armeria space and one for the other rooms of the museum. In detail, the first is a free-floating and unused space without internal gains for the whole year, as mentioned previously. Regarding the air infiltration, since the double lancet windows of Salone dell'Armeria are always closed, the *ACH* (Air Change Rate) is related just to the infiltration caused by air leakages through windows and the wooden roof. Therefore, the *ACH* was initially assumed equal to 0.1. Internal mass due to the presence of three transversal brick walls with a thickness of 45 cm was also taken into account, defining about 400 m² of brick surface exposed in the indoor environment, which increase the capability of retaining the water vapour.

For the other museum spaces, a standard internal load has been set according to the national building regulation [38]. The building operation profile of such spaces has been defined adopting the current condition. The infiltration rate adopted for those spaces is the same set for the Salone dell'Armeria, in the absence of further information.

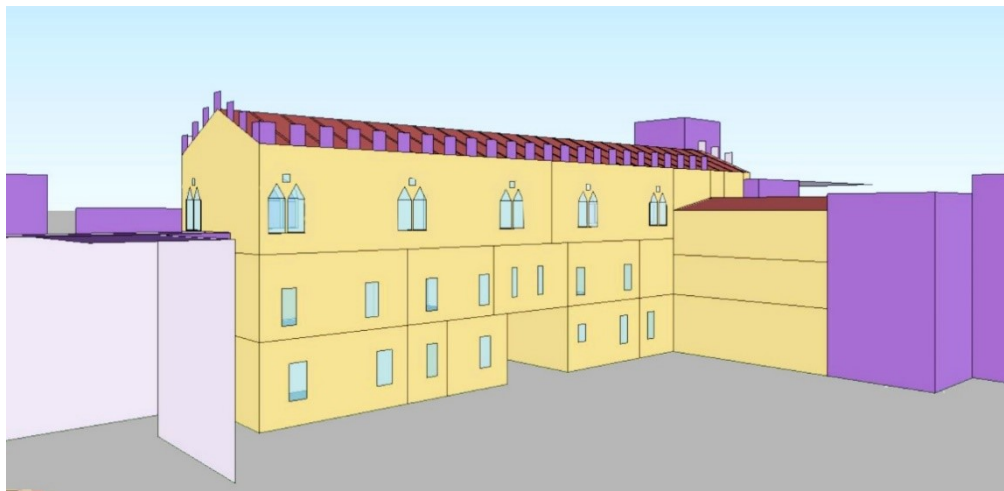


Figure 3. The energy model of Palazzo del Capitano with the Salone dell'Armeria (in yellow colour) and the rest of the Palazzo Ducale (in purple colour)

On-site ambient measurements

The assessment of the microclimatic performance was carried out to support the realization and the calibration/validation of the virtual model, able to reproduce realistic building behaviour.

In detail, the monitoring campaign was divided into two main phases:

- In the first phase, a series of measurements points were defined using pyrometers (infrared thermometer) and mobile temperature and humidity probes, which provided useful information for identifying the most representative measurement points;
- Based on the information obtained from the first surveys, two probes were installed in the second phase to acquire the continuous long-term data, in the positions shown in [Figure 4](#).

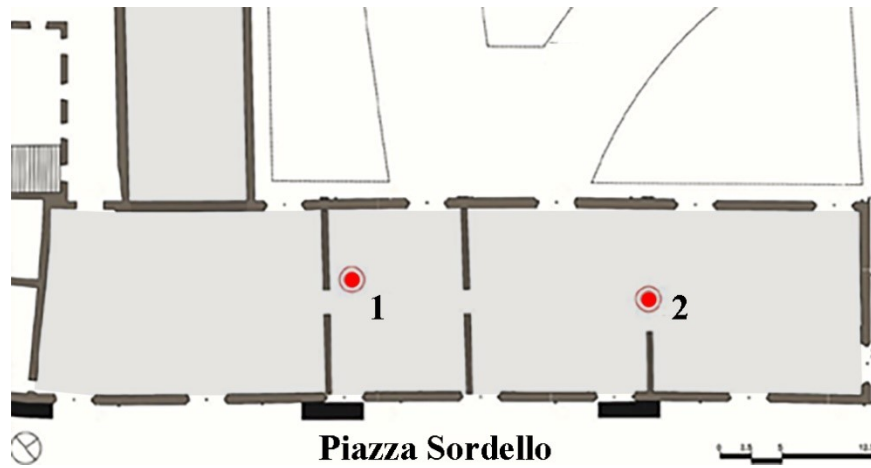


Figure 4. Position of the two long-term probes inside the Salone dell'Armeria

The hygrothermal properties of the Salone dell'Armeria were monitored for one year, starting from August 2017, with an hourly acquisition time step. Two Hobo MX Temp/RH data logger (MX1101) were placed in two significant points, about 12 m far from each other, at a height of about 3.50 m from the ground to avoid the influence of the solar radiation entering from windows. The main characteristics of the probes used are shown in **Table 2**.

Table 2. Main characteristics of the monitoring instrument

Instrument	Measured parameter	Measurement range	Accuracy	Resolution	Time response
HOBO MX Temp/RH Data Logger (MX1101)	Temperature	-20-70 °C	+/-0.21 °C (0 ... +50 °C)	0.024 °C (at 25 °C)	7:30 min. (air velocity equal to 1 m/s)
	Relative Humidity	1-90%	+/- 2% (20 ... 80%)	0.01%	20 sec. (at 90% RH with air velocity equal to 1 m/s)

Such instruments comply with the minimum requirements suggested by European regulations [39, 40] on the measurement of the microclimatic parameters for the conservation of cultural heritage. The differences between the two sensors are generally within +/-1 °C and +/- 5% for temperature and relative humidity respectively. The average value of the two probes was considered for the following assessment.

Figure 5 shows the indoor and outdoor air T and MR for the monitored period (from 1st August 2017 for one year) are reported.

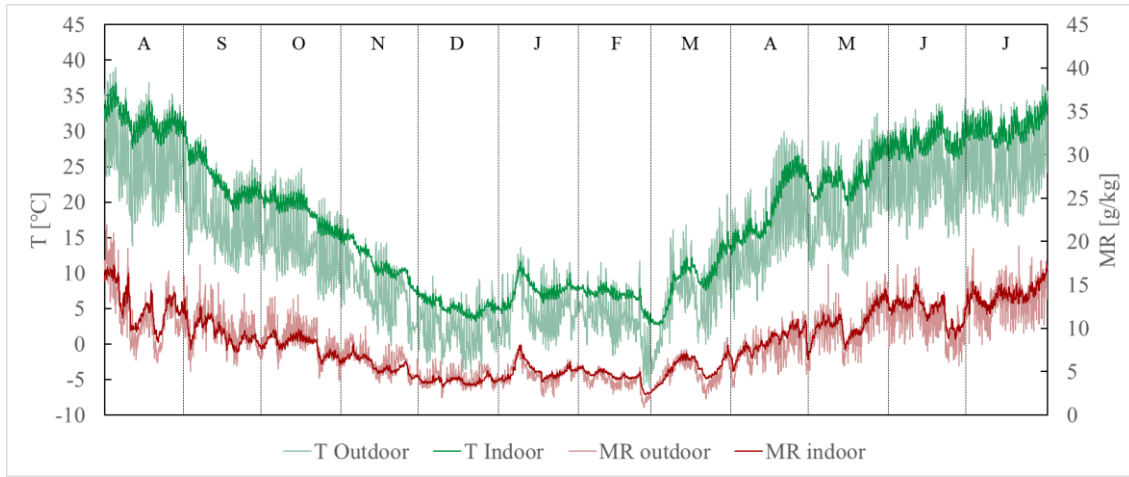


Figure 5. Indoor-outdoor temperature and mixing ratio

RESULTS AND DISCUSSION

First of all, the simulation was performed with the default algorithm set by EnergyPlus, the Effective Capacitance, with an *ACH* value of 0.11, which can be considered the optimal choice in relation to the calculated *MBE*, *MAE*, *RMSE* and R^2 equal to -0.25 g/kg, 0.63 g/kg, 0.79 g/kg respectively and 0.955 for the mixing ratio. Figure 6 shows the measured and simulated *MR* along the whole year using the EC model.

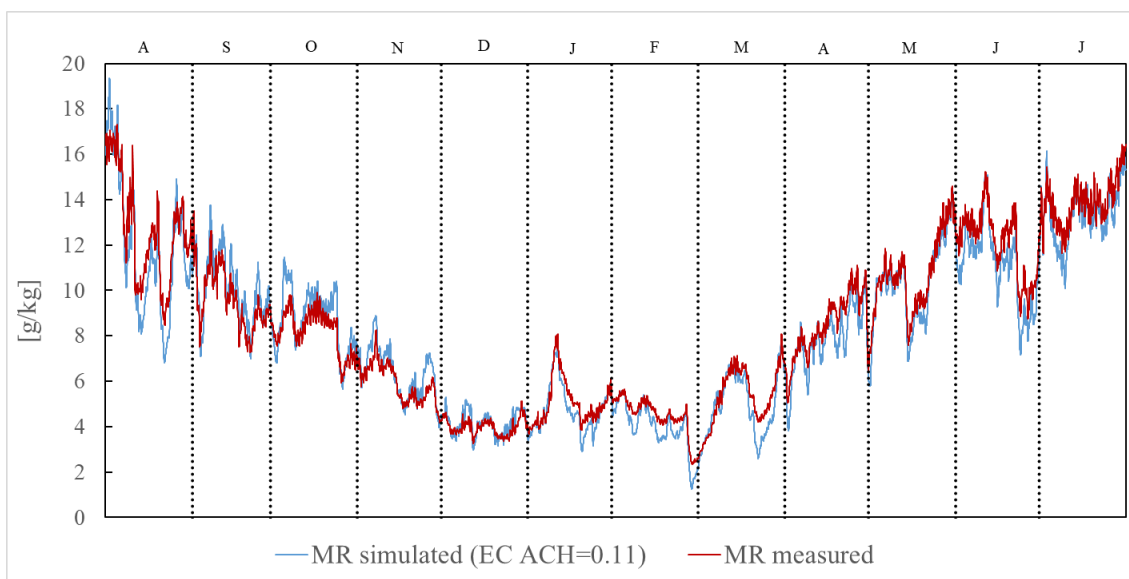


Figure 6. Mixing ratio simulated with EC model at 0.11 *ACH* and measured data

However, the default algorithm used by EnergyPlus has been changed with the effective EMPD model, since the EC model neglects the effect of moisture buffering, as previously mentioned.

It should be noted that the EMPD model requires some additional information such as the water vapour diffusion resistance factor, the coefficients “*a*”, “*b*”, “*c*”, and “*d*”, necessary to define the sorption isotherm curve used for building materials under equilibrium conditions, the surface/deep layer penetration depth and the vapour diffusion resistance factor of the coating layer. In the present work, such parameters have been set according to the EnergyPlus documentation and database [41], as reported in

Table 3.

Table 3. Moisture buffering properties of building materials for the EMPD model

Building material	Water vapour diffusion resistance factor	<i>a</i>	<i>b</i>	<i>c</i>	<i>d</i>	Surface layer penetration depth (m)	Deep layer penetration depth (m)
Brick	19.6	0.014	9.638	0.025	0.676	0.017	0.060
Concrete	6.6	0.045	0.352	0.086	14.8	0.008	0.030
Wood	150	0.204	2.320	0.430	72	0.001	0.004

After the implementation of the additional information required by the EMPD algorithm, a new simulation with the same *ACH* (0.11), previously considered calibrated, was performed. However, as shown in **Figure 7** the obtained *MR* values along the whole year do not fit well with the real monitored data.

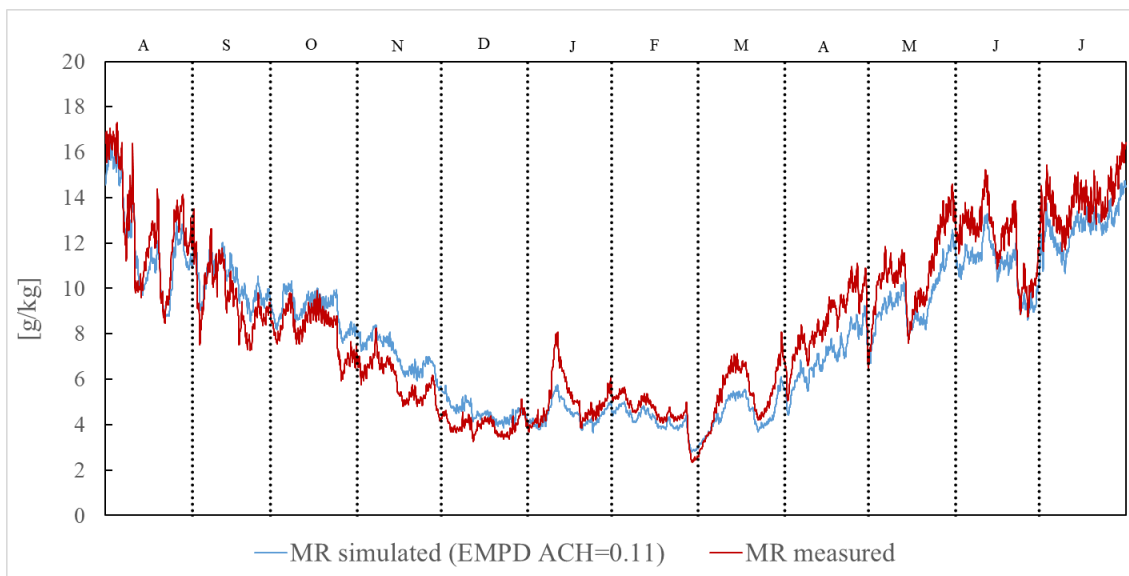


Figure 7. Mixing ratio simulated with EMPD model at 0.11 *ACH* and the measured data

In such regards, a new calibration has been carried out by the variation of the air change rate. As shown in **Table 4**, in the calibration process has been analysed seven simulations to achieve a good match with the measurements.

Table 4. Mixing ratio uncertainty indices calculated for different *ACH* values (with the EMPD model)

Simulation	<i>ACH</i> [1/h]	<i>MBE</i>	<i>MAE</i>	<i>RMSE</i>	<i>R</i> ²
1	0.11	-0.35	0.94	1.07	0.922
2	0.21	-0.32	0.76	0.88	0.974
3	0.28	-0.31	0.72	0.85	0.951
4	0.31	-0.31	0.71	0.85	0.951
5	0.41	-0.30	0.70	0.85	0.949
6	0.51	-0.29	0.70	0.87	0.946
7	0.71	-0.29	0.72	0.92	0.940

According to the different simulations (Table 4), the R^2 calculated for the MR parameter is particularly high in all cases, in a range between 0.922 and 0.974; on the contrary, the MBE , MAE and $RMSE$ are more variable. The MBE could be useful to understand the direction of the residuals and identify when the model is going to be calibrated (generally when the MBE became close to 0). In such respect, among the simulations carried out, the MBE is always negative, pointing that there is an overall slight overestimation of the simulated results.

The MAE and $RMSE$ indices differ from MBE due to their always positive results. The $RMSE$ is commonly higher than MAE , since the same is more sensitive to the amplitude of the residuals. The MAE has results less variable, between 0.70-0.72 in almost all the simulations. Therefore, the $RMSE$ can better represent the error variation, highlighting the amplitude of the residuals. Thanks to $RMSE$ it is possible to verify (see Table 4) that in simulation 7 the gap increases, even if the MAE does not change consistently.

In such respect, the $RMSE$ is used in Figure 8 to compare the simulation results with EC and $EMPD$ models for the different ACH values as shown in Table 4.

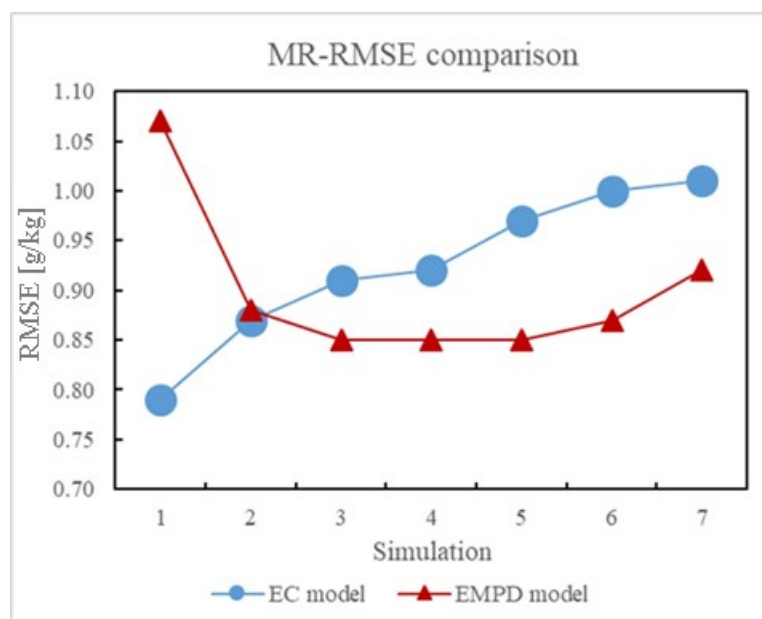


Figure 8. $RMSE$ calculated for MR according to the simulations with different ACH

As shown in Figure 8, the simulations with the lowest $RMSE$ for MR are numbers 3, 4 and 5, but the best result in terms of $RMSE$, MAE and R^2 is given by the simulation 4 (ACH equal to 0.31), which is about 3 times higher than the calibration previously obtained with the EC model. In this case (simulation 4 in Table 4), the values of MBE , MAE , $RMSE$ and R^2 are -0.31, 0.71, 0.85 and 0.951 respectively. In Figure 9, the measured and simulated MR for the whole year after the calibration with 0.31 ACH , has been shown.

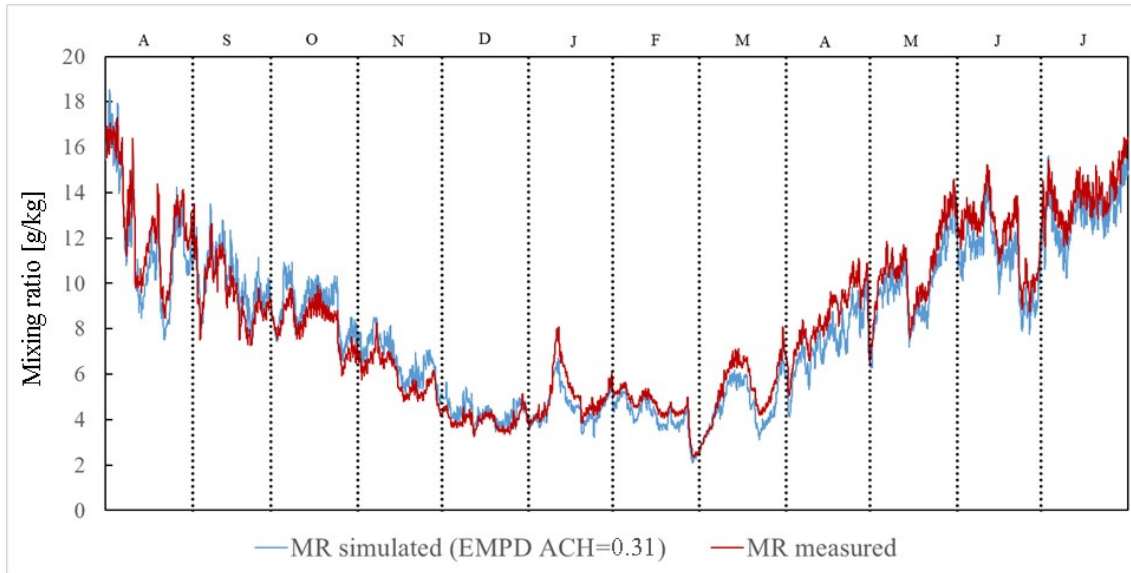


Figure 9. MR of the simulated model with EMPD model at 0.31 ACH and the measured data

In the context of preventive conservation of cultural heritage, the presence of thermal fluctuations (daily or seasonally) or high thermal levels compared to the conservation standard may cause expansion, acceleration of natural damage or chemical processes, increasing the fragility of organic artworks, etc. The thermal damage is often reversible, thus not highly dangerous for the objects. On the contrary, the humidity contained in the air has a pivotal role for the good preservation of several materials [42] because hygrometric fluctuations may produce irreversible damage and generate modifications in the size and shape of artefacts, as well as chemical reactions and biological deteriorations.

This suggests that, to further verify if the simulation model reproduces with adequate accuracy the relevant damage risks for hygroscopic materials [43, 44], the ratio between the number of simulated and measured cycles of RH (called prediction rate Q_v) can be calculated, according to the following formula:

$$Q_v = \frac{N_s}{N_m} \tag{5}$$

where N_s and N_m are respectively the numbers of times when the simulated and measured daily RH cycles exceed certain daily fluctuation variations (as the ranges shown in Table 5). Basically, the method evaluates the number of daily fluctuation cycles beyond different acceptability thresholds and calculate the ratio between the number of simulated and measured cycles. If this ratio deviates too far from 1, the reliability of the model decreases.

In this work, the Q_v ratio has been calculated with the MR parameter in order to evaluate how much the calibrated model reproduce a behaviour close to the reality compared to the initial settings (ACH=0.11). In Table 5 have been reported the calculated values of Q_v ratios as well as the number of times in which the daily MR cycles exceed the different thresholds according to the simulations with the EMPD model at 0.11 and 0.31 ACH.

Table 5. Assessment of the prediction rate Q_v and the number of daily cycles measured and simulated of MR for different ranges of variation

Daily MR fluctuation	Measured N_m	EMPD - ACH 0.11		EMPD- ACH 0.31	
		N_s	Q_v	N_s	Q_v
$(MR_{max} - MR_{min}) \leq 0.5$ g/kg	102	184	1.80	76	0.75

$(MR_{\max} - MR_{\min}) > 0.5 \text{ g/kg}$	263	181	0.69	289	1.10
$(MR_{\max} - MR_{\min}) > 1.0 \text{ g/kg}$	127	41	0.32	158	1.24
$(MR_{\max} - MR_{\min}) > 1.5 \text{ g/kg}$	38	11	0.29	64	1.68
$(MR_{\max} - MR_{\min}) > 2.0 \text{ g/kg}$	17	5	0.29	23	1.35

Such comparison demonstrates that the simulation with the EMPD model with an *ACH* of 0.11 provides many daily fluctuations completely different from the monitored data. In detail, it can be noted a high number of the daily cycles lower than 0.5 g/kg (184 times compared to the 102 monitored) due to the impact of the moisture buffering effect of the building materials which absorb the humidity from the air, with a consequent reduction of the mixing ratio. In such regard, the EMPD with a higher air change rate can better reproduce the real humidity daily fluctuations in the Salone dell'Armeria. The results reported in [Table 5](#) with an *ACH* of 0.31 (which is the value previously calibrated) show a number of daily fluctuations closer to the measurements and the calculated Q_v ratios are closer to the unit.

Finally, assuming to remove the three internal brick walls with their 400 m² of the exposed surface, the amplitude of the daily fluctuations of *MR* increases. In detail, the number of daily cycles for the smallest range of variation decreases (daily mixing ratio fluctuations $\leq 0.5 \text{ g/kg}$), while for the others it increases from 4% to 26%.

The results reported show the high impact of the moisture buffering model on the simulation output. The moisture buffering of materials acts as humidity storage, decreasing thus the *MR* peaks as well as the water content in the air, while a small variation of the external humidity content from outside air through infiltration suddenly changes the indoor *MR* in the default EC model.

Thus, the moisture buffering effect of building materials is particularly evident in historical buildings which are generally characterized by massive and porous constructions. More in detail, the moisture buffer effect of all hygroscopic materials in the indoor environment (e.g. interior surfaces of wall envelopes, the wooden roof, the floor, etc.) helps to absorb the vapour in the air when the indoor relative humidity is high and decrease indoor relative humidity.

On the contrary, when indoor relative humidity is low, these materials release the vapour back into the air and increase indoor relative humidity. Such phenomena, thus, moderate the variations of moisture content in the indoor air.

CONCLUSIONS

The effect of two different moisture buffering models in combination with air infiltration has been investigated in a historical building case study, using EnergyPlus software. The selected case study suits perfectly with the goal of the research since it is characterized by free-floating conditions and no internal gains, thus air infiltration can be considered the only moisture source and the building materials the only buffering contributors.

According to the obtained results, it can be said that the default model used by EnergyPlus (EC model) leads to an underestimation of the infiltration rate in comparison to the EMPD model, since hygrothermal interactions between the envelope and the environment are not considered or overestimated. The EMPD model would better predict the actual moisture capacitance of the indoor because it considers separately two moisture contents for the space and the interior surfaces of the building envelope.

As shown in this study, the model calibration allows reducing the gap between measurements and simulations, obtaining more accurate and reliable predictions. This is pivotal for the proper assessment of suitable solutions in terms of energy efficiency, comfort and conservation in the existing heritage buildings. Users shall be aware of the applicability of the different humidity models, trying to select the suitable one according to the specific conditions, to achieve the highest accuracy and more realistic results.

In such respect, the combined evaluation of different statistical indices can be considered a more effective approach to verify the model accuracy. The result obtained from the calibrated EMPD model provide an infiltration rate of about 3 times greater than the value of the default EC model. However, it should be noted that the EMPD model requires additional information about the hygroscopic properties of the materials which significantly affect the robustness of the results.

Understanding and taking into account the moisture buffering is necessary to ensure an accurate prediction of indoor humidity, but other important aspects of moisture modelling are present when considering indoor humidity and further investigation is necessary. In detail, the future research may include the quantification of the moisture buffering potential of furniture and different construction materials that characterize the envelope of historical buildings, the research of strategies or solutions that improve the moisture buffering and the spatial and temporal effect of occupants.

REFERENCES

1. Galatioto, G. Ciulla, R. Ricciu, An overview of energy retrofit actions feasibility on Italian historical buildings, *Energy*. 137 (2017) 991–1000. doi: <https://doi.org/10.1016/J.ENERGY.2016.12.103>.
2. M. Economidou, J. Laustsen, P. Ruyssevelt, D. Staniaszek, D. Strong, S. Zinetti, *Europe's buildings under the microscope*, 2011.
3. A. Martínez-Molina, I. Tort-Ausina, S. Cho, J.-L. Vivancos, Energy efficiency and thermal comfort in historic buildings: A review, *Renew. Sustain. Energy Rev.* 61 (2016) 70–85. doi: <https://doi.org/10.1016/J.RSER.2016.03.018>.
4. J. Ramos, L. Aires, The Effect of a Naturally Ventilated Roof on the Thermal Behaviour of a Building under Mediterranean Summer Conditions, *J. Sustain. Dev. Energy, Water Environ. Syst.* 8 (2020) 508–519. doi: <https://doi.org/https://doi.org/10.13044/j.sdewes.d7.0297>.
5. G.G. Akkurt, N. Aste, J. Borderon, A. Buda, M. Calzolari, D. Chung, V. Costanzo, C. Del Pero, G. Evola, H.E. Huerto-Cardenas, F. Leonforte, A. Lo Faro, E. Lucchi, L. Marletta, F. Nocera, V. Pracchi, C. Turhan, Dynamic thermal and hygrometric simulation of historical buildings: Critical factors and possible solutions, *Renew. Sustain. Energy Rev.* 118 (2020) 109509. doi: <https://doi.org/10.1016/j.rser.2019.109509>.
6. A. Buda, S. Mauri, Building survey and energy modelling: An innovative restoration project for casa del fascio in como, *ISPRS Ann. Photogramm. Remote Sens. Spat. Inf. Sci.* 42 (2019) 331–338. doi: <https://doi.org/10.5194/isprs-Archives-XLII-2-W11-331-2019>.
7. P. de Wilde, The gap between predicted and measured energy performance of buildings: A framework for investigation, *Autom. Constr.* 41 (2014) 40–49. doi: <https://doi.org/10.1016/J.AUTCON.2014.02.009>.
8. R.S. Adhikari, E. Lucchi, V. Pracchi, E. Rosina, Static and Dynamic Evaluation Methods for Energy Efficiency in Historical Buildings, in: *PLEA2013 - 29th Conf. Sustain. Archit. a Renew. Futur. Munich, Ger. 10-12 Sept. 2013*, 2013: pp. 10–12.
9. M. Calzolari, *Prestazione energetica delle architetture storiche: sfide e soluzioni: analisi dei metodi di calcolo per la definizione del comportamento energetico*, 1 (16 magg, ITA, 2018).
10. ANSI/ASHRAE, *Guideline 14-2014 -- Measurement of energy, demand, and water savings*, 2014.
11. A. Hamburg, K. Kuusk, A. Mikola, T. Kalamees, Realisation of energy performance targets of an old apartment building renovated to nZEB, *Energy*. 194 (2020) 116874. doi: <https://doi.org/10.1016/j.energy.2019.116874>.
12. R. Figueiredo, P. Nunes, M.C. Brito, Multiyear calibration of simulations of energy systems, *Energy*. 157 (2018) 932–939. doi:

- <https://doi.org/10.1016/j.energy.2018.05.188>.
13. A.L. Webb, Energy retrofits in historic and traditional buildings: A review of problems and methods, *Renew. Sustain. Energy Rev.* 77 (2017) 748–759. doi: <https://doi.org/10.1016/j.rser.2017.01.145>.
 14. A-Garrett, J. New, Scalable tuning of building models to hourly data, *Energy*. 84 (n.d.) 493–502. doi: <https://doi.org/10.1016/j.energy.2015.03.014>.
 15. J. Rouleau, L. Gosselin, P. Blanchet, Robustness of energy consumption and comfort in high-performance residential building with respect to occupant behavior, *Energy*. 188 (2019) 115978. doi: <https://doi.org/10.1016/j.energy.2019.115978>.
 16. N. Aste, S. Della Torre, R.S. Adhikari, M. Buzzetti, C. Del Pero, F. Leonforte, H.E.H. Cardenas, CFD Comfort Analysis of a Sustainable Solution for Church Heating, *Energy Procedia*. 105 (2017) 2797–2802. doi: <https://doi.org/10.1016/j.egypro.2017.03.603>.
 17. M. Qin, J. Yang, Evaluation of Different Thermal Models in EnergyPlus for Calculating Moisture Effects on Building Energy Consumption in Different Climate Conditions, *Build. Simul.* 9 (2016) 15–25. doi: <https://doi.org/10.1016/j.proeng.2015.09.194>.
 18. H. Yoshino, T. Mitamura, K. Hasegawa, Moisture buffering and effect of ventilation rate and volume rate of hygrothermal materials in a single room under steady state exterior conditions, *Build. Environ.* 44 (2009) 1418–1425. doi: <https://doi.org/10.1016/j.buildenv.2008.09.007>.
 19. O. Koronthalyova, The coupled effect of hygroscopic materials and ventilation regime on indoor humidity, in: IEA-EXCCO Energy Conserv. Build. Community Syst. Annex 41, 2014.
 20. N. Mendes, F.C. Winkelmann, R. Lamberts, P.C. Philippi, Moisture effects on conduction loads, *Energy Build.* 35 (2003) 631–644. doi: [https://doi.org/10.1016/S0378-7788\(02\)00171-8](https://doi.org/10.1016/S0378-7788(02)00171-8).
 21. J. Woods, J. Winkler, Effective moisture penetration depth model for residential buildings: Sensitivity analysis and guidance on model inputs, *Energy Build.* 165 (2018) 216–232. doi: <https://doi.org/10.1016/j.enbuild.2018.01.040>.
 22. M. Jarić, N. Budimir, M. Pejanović, I. Svetel, A Review of Energy Analysis Simulation Tools, in: 7th Int. Work. Conf. "Total Qual. Manag. – Adv. Intell. Approaches", 2013.
 23. U.S.D. of Energy, EnergyPlus Version 9.1.0 Documentation - Engineering Reference, 2016.
 24. M. Woloszyn, C. Rode, A.S. Kalagasidis, A. Janssens, M. De Paepe, From EMPD to CFD - Overview of different approaches for heat air and moisture modeling in IEA annex 41, *ASHRAE Trans.* 115 PART 2 (2009) 96–110.
 25. J. Woods, J. Winkler, D. Christensen, Evaluation of the Effective Moisture Penetration Depth Model for Estimating Moisture Buffering in Buildings, 2013.
 26. T. Yan, Z. Sun, X. Xu, H. Wan, G. Huang, Development of a simplified dynamic moisture transfer model of building wall layer of hygroscopic material, *Energy*. 183 (2019) 1278–1294. doi: <https://doi.org/10.1016/j.energy.2019.07.033>.
 27. G. Mustafaraj, J. Chen, G. Lowry, Development of room temperature and relative humidity linear parametric models for an open office using BMS data, *Energy Build.* 42 (2010) 348–356. doi: <https://doi.org/10.1016/j.enbuild.2009.10.001>.
 28. G. Ruiz, C. Bandera, Validation of Calibrated Energy Models: Common Errors, *Energies*. 10 (2017). doi: <https://doi.org/10.3390/en10101587>.
 29. G. Steindl, W. Kastner, V. Stangl, Comparison of Data-Driven Thermal Building Models for Model Predictive Control, *J. Sustain. Dev. Energy, Water Environ. Syst.* 7 (2019) 730–742. doi: <https://doi.org/https://doi.org/10.13044/j.sdewes.d7.0286>.
 30. O. Timur, K. Zor, Ö. Çelik, A. Teke, İ. Turgay, Application of Statistical and Artificial Intelligence Techniques for Medium-Term Electrical Energy Forecasting: A Case Study for a Regional Hospital, *J. Sustain. Dev. Energy, Water Environ. Syst.* 8 (2020) 520–536. doi: <https://doi.org/https://doi.org/10.13044/j.sdewes.d7.0306>.

31. ANSI/ASHRAE, ASHRAE Guideline 14-2002 Measurement of Energy and Demand Savings, 2002.
32. Efficiency Valuation Organization, International Performance Measurement and Verification Protocol: Concepts and Options for Determining Energy and Water Savings Volume 1, Washington, DC, USA, 2012. doi: <https://doi.org/10.1126/science.15.390.961>.
33. H.E. Huerto-Cardenas, F. Leonforte, N. Aste, C. Del Pero, G. Evola, V. Costanzo, E. Lucchi, Validation of dynamic hygrothermal simulation models for historical buildings: State of the art, research challenges and recommendations, *Build. Environ.* 180 (2020) 107081. doi: <https://doi.org/10.1016/j.buildenv.2020.107081>.
34. F. Leonforte, C. Del Pero, N. Aste, B. Buzzetti, H.E. Huerto-Cardenas, H. El Khatib, The pivotal role of moisture buffering effect in energy simulation of historic buildings, in: 14th Conf. Sustain. Dev. Energy, Water Environ. Syst., Dubrovnik, 2019.
35. UNI, UNI 10351 - Materiali da costruzione. Conduttività termica e permeabilità al vapore, 1994.
36. International Organization for Standardization (ISO), Building materials and products. Hygrothermal properties. Tabulated design values and procedures for determining declared and design thermal values, Standard ISO 10456, (2007).
37. D. Milone, G. Peri, S. Pitruzzella, G. Rizzo, Are the Best Available Technologies the only viable for energy interventions in historical buildings?, *Energy Build.* 95 (2015) 39–46. doi: <https://doi.org/10.1016/j.enbuild.2014.11.004>.
38. Ente Nazionale Italiano di Unificazione (UNI), Prestazioni energetiche degli edifici. Parte 1: Determinazione del fabbisogno di energia termica dell'edificio per la climatizzazione estiva ed invernale, Standard UNI 11300, UNI, Milano, 2014., (2014).
39. CEN, EN 15758: 2010 – Conservation of cultural property. Procedures and instruments for measuring temperatures of the air and the surfaces of objects., 2010.
40. CEN, EN 16242: 2012 – Conservation of cultural heritage – Procedures and instruments for measuring humidity in the air and moisture exchanges between air and cultural property., 2012.
41. EnergyPlus, Input Output Reference, *Encycl. Ref. to EnergyPlus Input Output.* (2010).
42. N. Aste, R.S. Adhikari, M. Buzzetti, S. Della Torre, C. Del Pero, H.E. Huerto C, F. Leonforte, Microclimatic monitoring of the Duomo (Milan Cathedral): Risks-based analysis for the conservation of its cultural heritage, *Build. Environ.* 148 (2019) 240–257. doi: <https://doi.org/10.1016/j.buildenv.2018.11.015>.
43. R. Kilian, Klimastabilität historischer Gebäude, *Bewertung hygrothermischer Simulationen im Kontext der Präventiven Konservierung*, 2013.
44. V. Rajčić, A. Skender, D. Damjanović, An innovative methodology of assessing the climate change impact on cultural heritage, *Int. J. Archit. Herit.* 12 (2018) 21–35. doi: <https://doi.org/10.1080/15583058.2017.1354094>



Paper submitted: 10.06.2020
Paper revised: 02.09.2020
Paper accepted: 09.10.2020